Effect of strontium and cooling rate upon eutectic temperatures of A319 aluminum alloy

Enrique Javier Martínez Delgado, Miguel Ángel Cisneros Guerrero, Salvador Valtierra, Jacques Lacaze

Effect of strontium and cooling rate upon eutectic temperatures of A319 aluminum alloy

E.J. Martínez D, M.A. Cisneros G, S. Valtierra and J. Lacaze
Instituto Tecnológico de Zacatecas, Depto. Metal-Mecánica, Carretera Panamericana, Entronque a Guadalajara S/N, 98 000,IZacatecas Zac., México
Instituto Tecnológico de Saltillo, Depto. Metal-Mecánica, Blvd. V. Carranza 25280, Saltillo, Coahuila, México
Nemak S.A. de C.V., R&D, Monterrey N.L. 66 000, México
CIRIMAT, ENSIACET, 31077 Toulouse Cedex 4, France
Received 27 September 2004; revised 1 November 2004; accepted 15 November 2004.
Available online 8 December 2004.

Abstract

DTA analysis was used to investigate the solidification reactions of alloy A319 with either 12 or 136 ppm of Sr added. Strontium does not affect primary solidification of (Al) dendrites but modifies the kinetics of the (Al)–Si eutectic. The effects of Sr level and of cooling rate on the characteristic temperatures for the (Al)–Si and other eutectic reactions are described.

Keywords: Solidification; Differential thermal analysis (DTA); Aluminum alloy A319; Strontium modification

1. Introduction
2. Experimental details
3. Results and discussion
4. Conclusions
Acknowledgements
References

1. Introduction

Alloy A319 is essentially a hypoeutectic Al–Si alloy with two main solidification stages, formation of aluminum rich (Al) dendrites followed by development of two-phase (Al)–Si eutectic. However, the presence of additional alloying elements such as Mg and Cu, as well as of impurities such as Fe and Mn, leads to a more complex solidification sequence. Accordingly, the as-cast microstructure of A319 alloy presents many inter-metallic phases in addition to (Al) and Si ones. The formation of these phases should correspond to successive reactions during solidification with an increasing number of phases involved at decreasing temperature. In practice, Bäckerud et al. [1] identified five reactions in alloy 319.1 with at most four solid phases as listed in Table 1. For a similar alloy, Samuel et al. [2] preferred to indicate the new solid phase(s) appearing at each characteristic temperature as given also in Table 1. The compositions of both alloys are listed in Table 2. To determine the characteristic temperatures, Bäckerud et al. [1] used differential scanning calorimetry (DSC) while Samuel et al. [2] mainly used thermal analysis (TA).

Table 1.

Reactions occurring during solidification of some 319 alloys according to Bäckerud et al. [1] and to Samuel et al. [2]

Backerud et al. [1]	**Temperature (°C)**	**Samuel et al. [2]**	**Temperature (°C)**
(Al) dendritic network	609	(Al) dendritic network	610
Liq. → (Al) + $Al_{15}Mn_3Si_2$ + (Al_5FeSi)	590		
Liq. → (Al) + Si + Al_5 FeSi	575	Precipitation of eutectic Si	562
		Precipitation of $Al_6Mg_3FeSi_6$ + Mg_2Si	554
Liq. → (Al) + Al_2Cu + Si + Al_5FeSi	525	Precipitation of Al_2Cu	510
Liq. → (Al) + Al_2Cu + Si + $Al_5Mg_8Cu_2Si_6$	507	Precipitation of $Al_5Mg_8Cu_2Si_6$	490

Table 2.

Chemical composition of the alloys mentioned in this paper (wt.% except for Sr)

	Si	**Cu**	**Fe**	**Mn**	**Mg**	**Ti**	**Sr (ppm)**
Bäckerud et al. [1]	5.7	3.4	0.62	0.36	0.10	0.14	–
Samuel et al. [2]	6.23	3.8	0.46	0.14	0.06	0.14	–
Mulazimoglu [3]	5.9	3.3	0.21	<0.02	0.01	0.02	–
This study, low Sr alloy	7.31	3.27	0.64	0.42	0.29	0.07	12
This study, high Sr alloy	7.23	3.33	0.62	0.42	0.30	0.08	136

As shown Table 1, the two solidification sequences differ only slightly. After primary deposition of (Al) dendrites, Bäckerud et al. [1] detected the precipitation of $Al_{15}Mn_3Si_2$ (possibly together with Al_5FeSi) which was not observed by Samuel et al. [2] presumably because of the smaller Mn content of the alloy used by these latter authors (Table 2). The temperature for precipitation of the (Al)–Si eutectic differs significantly in these studies, 575 °C for Bäckerud et al. [1] and 562 °C for Samuel et al. [2] in agreement with the fact that this temperature is depressed by increasing the nominal Si content of the alloy. A slight thermal arrest at 554 °C corresponding to the precipitation of $Al_6Mg_3FeSi_6$ and Mg_2Si could be detected by Samuel et al. [2] by comparison to their results on B319.1 alloy with a high Mg content (0.5 wt.%) in which this reaction was easily observed. This reaction as well as the two corresponding phases were not observed by Backerud et al. [1].

The Al_2Cu phase is often observed to precipitate both in a blocky shape and in fine multi-phase eutectic-like deposits [2] and [3]. These two shapes may be observed in castings cooled at very different rates, with apparently a lower proportion of blocky precipitates as the cooling rate are increased [2]. Samuel et al. [2] reported that distinct thermal arrests related to these two forms

could be recorded only at low cooling rates, and suggested that the reaction at higher temperature (510 °C in Table 1) should be associated to the blocky shape. Interestingly enough, the start of precipitation of Al_2Cu has been reported to occur at very different temperatures, from 549 °C [3] down to 510 °C [2]. However, it seems quite unlikely that Al_2Cu could precipitate at a temperature higher than the eutectic (Al)–Al_2Cu in the binary Al–Cu system (548 °C) [4].

The four phase (Al) + Al_2Cu + Si + Al_5FeSi reaction at 525 °C has been recorded by Bäckerud et al. [1] and by Mulazimoglu et al. [3] when other authors did not detect it [2] and [5]. While this reaction relates to the start of Al_2Cu precipitation according to Backerud et al. [1], Mulazimoglu et al. [3] associated it to the fine multi-phase eutectic-like deposit with Al_2Cu. According to Samuel et al. [2], this multi-phase deposit should rather involve $Al_5Mg_8Cu_2Si_6$ together to Al_2Cu, somewhat in agreement with Backerud et al. [1].The phase $Al_5Mg_8Cu_2Si_6$ appears in an invariant eutectic of the quaternary Al–Cu–Mg–Si system which corresponds to the last reaction listed by Backerud et al. [1] (Table 1). The equilibrium temperature of this reaction is 507 °C [4], but it presents some systematic undercooling upon solidification [6].

Another degree of complexity in the understanding of the solidification sequence of alloy A319 is due to the addition of eutectic modifier such as strontium. This modification is obtained through a dramatic change of the shape of the silicon particles and is related to a modification of the growth of the (Al)–Si eutectic. Such an effect should be detectable by thermal analysis, and this has led to studies to define melt control procedures [7]. At a given cooling rate, Sr decreases nucleation and growth temperatures of the (Al)–Si eutectic and this effect is higher the higher the cooling rate [5] and [7]. Also, adding Sr does not affect primary deposition of (Al) but apparently modifies reactions occurring after the (Al)–Si precipitation [7]. Sokolowski et al. [8] showed that 100 ppm Sr increases the temperature of the last two reactions in Table 1, respectively from 505 °C to 513 °C and 496 °C to 501 °C in their experiments. This is in contradiction to the conclusion of Samuel et al. [2] on the basis of DSC experiments upon heating samples without Sr and with 300 ppm Sr. It should be emphasized that in these latter experiments the final eutectic had apparently been dissolved by solid-state diffusion during heating so that the start of melting was recorded at much higher temperature than expected from cooling records.

This short survey shows it should be of great interest to further study the effect of Sr addition and cooling rate on the solidification sequence of A319 alloy. This paper presents experimental results obtained by means of differential thermal analysis (DTA) for two levels of Sr addition (12 and 136 ppm) and three scanning rates (2, 10 and 20 °C/min).

2. Experimental details

Metal was processed as described previously by Paramo et al. [5], degassed with nitrogen injection, refined with TiB_2 and modified with an Al–Sr master alloy. Two levels of Sr addition, 12 ppm and 136 ppm were achieved. These alloys were then cast at 760 °C in cylindrical sand moulds with large risers to avoid any defects in the parts. Samples were then machined to bars 6 mm in diameter and 100 mm in length. The final compositions of the corresponding two alloys are given in Table 2. The micrographs in Fig. 1 clearly illustrate that the (Al)–Si eutectic is much finer with the largest Sr addition. Both alloys were subjected to differential thermal analysis using a SETSYS apparatus from SETARAM. The DTA signal was recorded on heating and cooling at three scanning rates, 2, 10 and 20 °C/min. The scanning rate was the same for heating and cooling and a new sample was used for each run. After a sample has been introduced in the measurement cell, this latter was evacuated and filled with argon twice. A low argon flux was then fixed and heating started. The DTA samples thus obtained were afterwards prepared for metallographic observations.

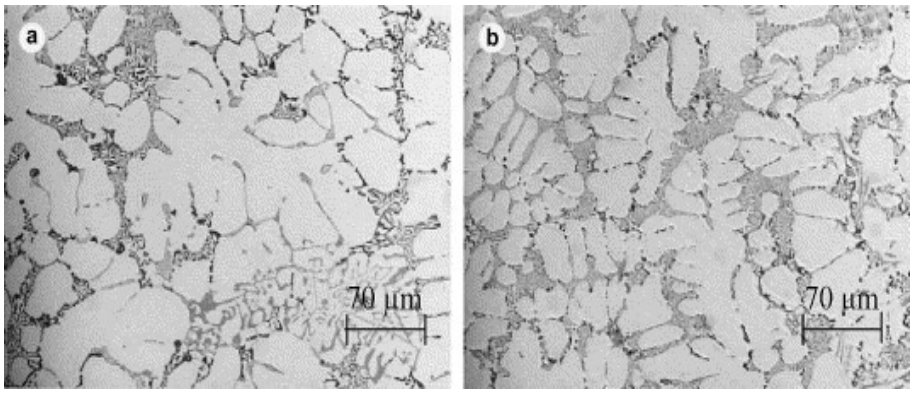

Fig. 1. Micrographs of as-cast alloys: (a) alloy with 12 ppm Sr and (b) alloy with 136 ppm Sr.

3. Results and discussion

Fig. 2a and b show the DTA thermograms obtained upon cooling of samples from the low Sr and high Sr alloys respectively. Three main peaks show up on every record that correspond at decreasing temperature to: (i) precipitation of (Al) dendrites; (ii) nucleation and growth of (Al)–Si eutectic; (iii) precipitation of multiphase eutectic $\alpha Al + Al_2Cu + Si + Al_5Mg_8Cu_2Si_6$. For both alloys, the first thermal arrest is very sharp showing that (Al) dendrites formed with some undercooling and then grew very rapidly. After this initial step, it is observed that the shape of the thermograms depends on the cooling rate. At 2 °C/min, the DTA signal decreases to a small value within a temperature interval of about 5 °C, while at 20 °C/min this decrease is much more limited. This indicates that a significant fraction of (Al) is still depositing in this latter case when nucleation of the (Al)–Si eutectic begins.

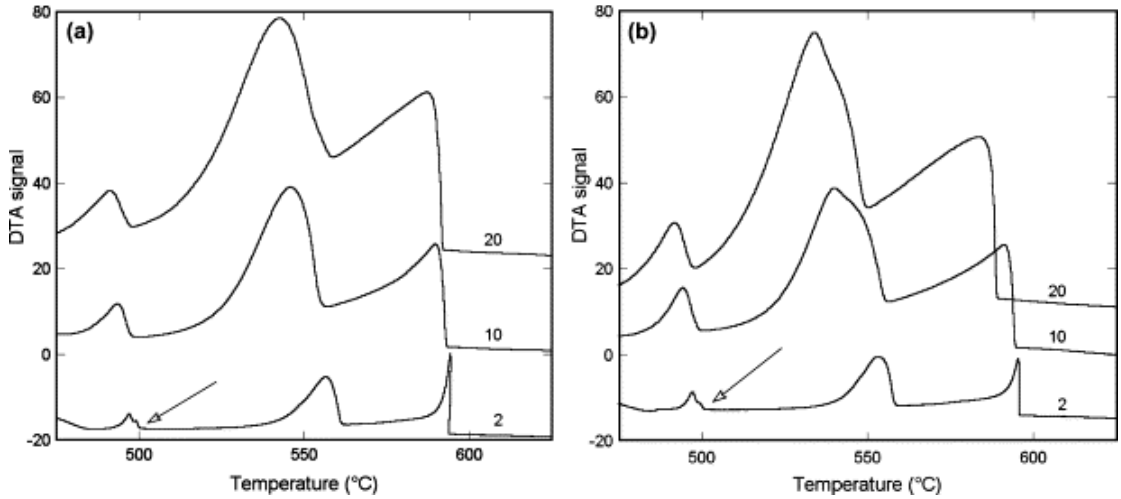

Fig. 2. DTA thermograms recorded during cooling at 2, 10 and 20 °C/min: (a) low Sr alloy and (b) high Sr alloy.

The thermal arrest corresponding to the (Al)–Si eutectic appears to be affected by the Sr level: after an initial rapid growth, the decrease of latent heat release is much more marked at high Sr than at low Sr level. In agreement with published literature, this effect of modification appears more clearly as the cooling rate is increased [9]. On the contrary, the last thermal arrest appears similar irrespective of the Sr level. The salient feature is that a small initial hump shows up at the

base of the peak for the lowest cooling rate for both alloys (arrow in the graph), much in line with the observations made on TA records by Samuel et al. [2]. Further analysis of the DTA thermograms was performed by picking up characteristic temperatures of the two eutectic reactions. This has been done also on the records obtained on heating which all showed the same three main peaks. For cooling records, the start and peak temperatures were used while for heating records only the peak temperatures were considered. These data are reported in Fig. 3 as a function of the square root of the scanning rate, with open symbols for low Sr alloy and solid symbols contrariwise. Because of heat transfer resistance [10], it is expected that any characteristic temperature should apparently increase with increase of the heating rate with respect to the equilibrium temperature and vice versa. This is illustrated with empty squares in Fig. 3 that represent the peak temperature of the (Al)–Si reaction in the low Sr alloy. The data can be satisfactorily extrapolated to a single temperature at zero scanning rates, the value of which is 565 °C. While the peak temperatures for high Sr alloy (solid squares) are in perfect agreement with those for low Sr alloy in the case of heating records, they are significantly lower for cooling than the peaks for the low Sr alloy, this difference is about 5 °C, a value similar to the change of the eutectic plateau temperature recorded in TA [2]. Data for the start of the (Al)–Si eutectic upon cooling (circles) do not show a clear trend with either cooling rate or Sr content. Further study on this should be of great interest in order to clarify if this is due to some variability in the nucleation process of Si or if this could be accounted for by solidification kinetics and related microsegregation build-up during primary (Al) precipitation.

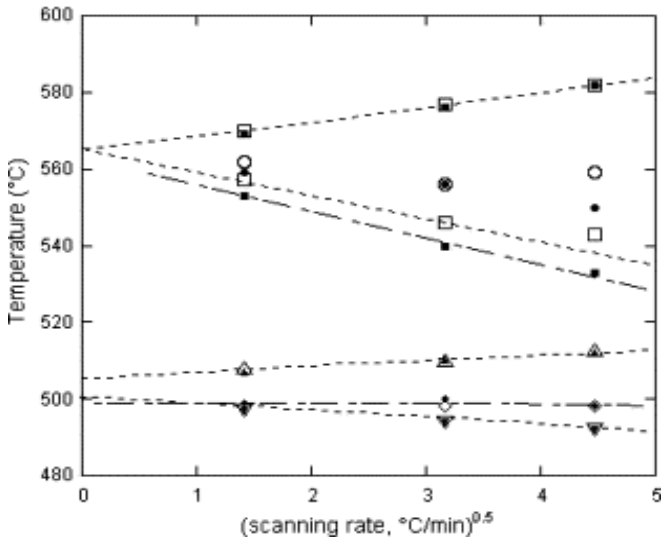

Fig. 3. Effect of scanning rate on the characteristic eutectic temperatures (see text for the meaning of the symbols).

Triangles show the peak temperatures of the final eutectic reaction. It is seen that these temperatures are not affected by Sr content, empty and solid symbols being superimposed for all scanning rates. This is in contradiction to the results from Sokolowski et al. [8] while agreeing with those by Samuel et al. [2]. The interesting feature is that extrapolating the data upon heating and cooling to a zero scanning rate gives two differing temperatures, respectively 505 °C and 501 °C. This temperature difference is tentatively associated to the minimum undercooling necessary to nucleate the new solid phase(s) that should appear in the terminal eutectic upon solidification. This amount of undercooling agrees with the value previously reported for the similar reaction in the quaternary Al–Cu–Mg–Si system [6]. Interestingly enough, the extrapolated temperature of 501 °C corresponds to the temperature of the initial hump on the DTA records at 2 °C/min. Also, it is seen that the temperature for the start of the reaction upon cooling, plotted with diamonds, is only slightly sensitive to cooling rate and that the

corresponding data could be extrapolated to a slightly lower temperature than 501 °C, about 499 °C in Fig. 3.

The last step of analysis of the DTA records was to look for slight slope changes which could indicate that some other reactions could be detected. Such a detailed analysis of the thermograms may be improved by using the derivative of the records. Fig. 4 presents both the DTA record and its derivative in the case of high Sr alloy cooled at 10 °C/min. It is seen that a clear arrest could be associated with the shoulder on the signal related to the (Al)–Si eutectic. A similar arrest could be found at a cooling rate of 20 °C/min while the DTA signal is too smooth at 2 °C/min to allow any unambiguous interpretation. The temperature of this arrest is 544 °C and 540 °C at respectively 10 and 20 °C/min. A similar arrest was also observed at 555 °C on low Sr alloy cooled at 20 °C/min, and nothing could be detected for the other cooling rates. These temperatures could correspond to the formation of $Al_6Mg_3FeSi_6$ and Mg_2Si according to Samuel et al. [2].

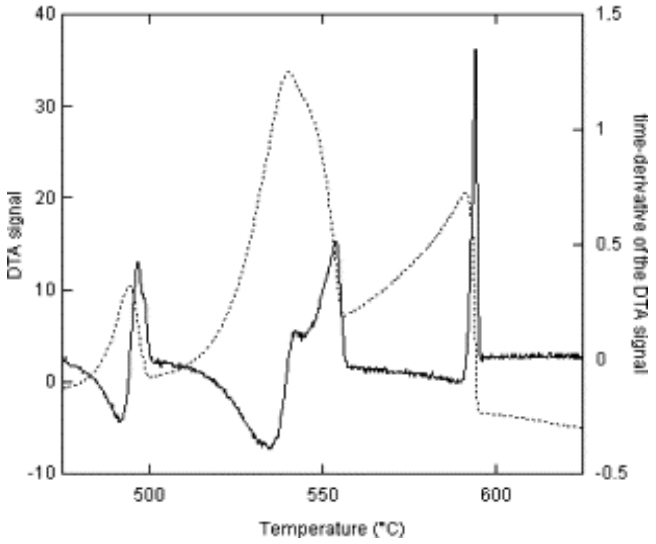

Fig. 4. DTA thermogram and its derivative for high Sr alloy cooled at 10 °C/min.

Based on the shape and contrast of the phases, it was found that most of the phases listed in Table 1 could be observed in the DTA samples but $Al_6Mg_3FeSi_6$. Modification of the (Al)–Si eutectic was not evidenced and this agrees with Tenekedjiev and Gruzleski [7] who found that at low cooling rate the effect of Sr addition can be observed on TA records without showing up in the microstructure. Also, Al_2Cu was seen to appear with both a blocky shape and associated within a fine multi-phase deposit. Owing to the high amount of Al_2Cu with respect to other minor phases, it is clear that the last eutectic reaction in the DTA records relates to its precipitation. Thus, if the hump on this last peak is associated to the formation of the blocky Al_2Cu phase in a divorced eutectic, it may be suggested that these precipitates develop until the temperature is low enough for coupled growth to set up. Increase of the cooling rate decreases the time let for independent growth of Al_2Cu precipitates and thus to a decrease of their volume fraction as experimentally observed [2]. Increase of the cooling rate also limits the possibility to record two separate thermal arrests corresponding respectively to the formation of Al_2Cu blocky precipitates and to the set-up of the final eutectic reaction.

4. Conclusions

The similarity between DTA thermograms obtained on low and high Sr A319 alloy at given cooling rates is striking, showing that Sr addition has a direct influence only on the growth

mechanism of the (Al)–Si eutectic. Possible effect on the nucleation step of this eutectic would need further study, in particular would require to consider primary solidification of (Al) dendrites. As a matter of fact, one may expect that small changes of overall eutectic kinetics due to Sr modification could help understanding subtle modifications during final stages of solidification as well as in the precipitation of iron and manganese rich phases.

Acknowledgments

Thanks are due to COSNET and to the ECOS-ANUIES program (contract number M99-P04) for support of this project.

References

L. Bäckerud, G. Chai and J. Tamminen, *AFS/SKANALUMINIUM* **71** (1990), p. 229.

F.H. Samuel, A.M. Samuel and H.W. Doty, *AFS Trans* **104** (1996), p. 893.

M.H. Mulazimoglu, N. Tenekedjiev, B.M. Closset and J.E. Gruzleski, *Cast Metals* **6** (1993), p. 16.

Phillips HWL. Annotated equilibrium diagrams of some aluminium alloy systems. The Inst. Metals, report no. 25, 1959.

V. Paramo, R. Colas, E. Velasco and S. Valtierra, *Mater Eng Perform* **9** (2000), p. 616.

J. Lacaze, G. Lesoult, O. Relave, I. Ansara and J.P. Riquet, *Z. Für Metallkunde* **78** (1987), p. 141.

N. Tenekedjiev and J.E. Gruzleski, *AFS Trans* **99** (1991), p. 1.

J.H. Sokolowski, M.B. Djurdjevic, C.A. Kierkus and D.O. Northwood, *J Mater Process Technol* **109** (2001), p. 174.

Gruzleski JE, Closset BM. American Foundrymen's Society Inc., 1990; p. 54.

W.J. Boettinger and U.R. Kattner, *Metall Mater Trans A* **33** (2002), p. 1779.

Corresponding author. Tel.: +52 492 923 8011; fax: +52 492 924 5366